ELSEVIER

CrossMark

Multi-group formulation of the temperature-dependent resonance scattering model and its impact on reactor core parameters

Shadi Z. Ghrayeb [a], Abderrafi M. Ougouag [b,*], Mohamed Ouisloumen [c], Kostadin N. Ivanov [a]

[a] Department of Mechanical and Nuclear Engineering, The Pennsylvania State University, 230 Reber Building, University Park, PA 16802, USA
[b] Idaho National Laboratory, MS-3860, PO Box 1625, Idaho Falls, Idaho 83415, USA
[c] Westinghouse Electric Company, 1000 Westinghouse Drive, Cranberry Township, PA 1606, USA

Guillermo Ibarra

Nuclear Engineering Research Seminar, March 24th, 2020

$$\Sigma_t(E')\phi(E') = \int_0^\infty P(E \to E')\sigma_s(E)\phi(E)dE$$

$$\Sigma_t(E')\phi(E') = \int_0^\infty P(E \to E')\sigma_s(E)\phi(E)dE$$

$$\Sigma_t(E')\phi(E') = \int_{E'}^{E'/\alpha} \frac{\sigma_s(E)}{(1-\alpha)E}\phi(E)dE$$

$$\sigma_s(E)P(E \to E') = \begin{cases} \frac{\sigma_s(E)}{E(1-\alpha)}, & \alpha E \le E' \le E, \\ 0, & otherwise. \end{cases}$$

History of the Resonance Scattering Model

- Ouisloumen and Sanchez (1990) - RSM
- Rothenstein, 2004; Dagan, 2004 - $S(\alpha, \beta)$ tables
- Becker et al. (2009b) - Doppler broadened rejection correction (DBRC) approach

Table 1
Summary of results performed using the resonance scattering model applied to the Mosteller benchmark.

#	Researcher(s)	Energy range	Nuclei	Method	CODE	LIBRARY	Fuel	Δk (pcm)	FTC diff. (%)[1]
1	Becker et al., 2009c	<210 eV	^{238}U	SVT vs. DBRC	MCNP5	JEFF3.1	UOX	–	8–16[2]
				SVT vs. DBRC			MOX[a]		
				SVT vs. DBRC			MOX[b]		
2	Sunny et al., 2012	<210 eV	^{238}U	DBRC	MCNP5	ENDF/B-VII	UOX	6 ± 25–194 ± 40	4.2 ± 0.3–15.2 ± 1.0
3	Sunny 2013	<210 eV	^{238}U	DBRC	MCNP5	ENDF/B-VII	UOX	20 ± 40–271 ± 41	8.8 ± 0.6–25.1 ± 1.7
4	Mori and Nagaya, 2009	>4.5 eV	^{238}U, ^{235}U	ASY vs. WCM	MVP-2	JENDL-3.3	UOX	72 ± 8–222 ± 14	7.2 ± 0.1–11.7 ± 0.2
5	Zoia et al., 2013	<210 eV	^{238}U	SVT vs. DBRC	TRIPOLI-4	ENDF/B-VII	UOX	66 ± 13–225 ± 14	6.2 ± 0.2–12.8 ± 0.3
6		<210 eV	^{238}U	SVT vs. WCM		ENDF/B-VII	UOX	77 ± 13–274 ± 18	8.7 ± 0.2–15.6 ± 0.4
7		0.1 eV–1 keV	^{238}U	SVT vs. DBRC		CEAV5.1	UOX	59 ± 6–232 ± 7	9.6 ± 0.1–12.7 ± 0.2
8		0.1 eV–1 keV	All nuclei	SVT vs. DBRC		CEAV5.1	UOX	62 ± 6–233 ± 7	9.3 ± 0.1–12.4 ± 0.1
9		0.1 eV–1 keV	^{238}U	SVT vs. DBRC		CEAV5.1	MOX[a]	67 ± 7–177 ± 6	7.0 ± 0.1–9.1 ± 0.1
10		0.1 eV–1 keV	All nuclei	SVT vs. DBRC		CEAV5.1	MOX[a]	108 ± 7–222 ± 6	8.0 ± 0.1–11.2 ± 0.1
11		0.1 eV–1 keV	Actinides	SVT vs. DBRC		CEAV5.1	MOX[a]	113 ± 7–232 ± 6	7.5 ± 0.1–11 ± 0.1
12	Ono et al., 2012	4–200 eV	Not specified	Deterministic	Not specified	Not specified	UOX	50–200	9.3–10.1[3]
13		4–200 eV					MOX[a]	70–160	6.5–7.2[4]
14	Lee et al., 2009	<1000 eV	^{238}U	ASY vs. WCM	CASMO-5[5]	ENDF/B-VII	UOX	59–212	9.2–9.8
15	Ghrayeb et al.	<20 MeV	Actinides	Deterministic	DRAGON	ENDF/B-VII	UOX	68–208	8.6–9.8
16	(current work)	<20 MeV	^{238}U				UOX	68–205	8.6–9.7
17		<20 MeV	^{238}U				MOX[a]	74–165	6.2–7.9
18		<20 MeV	Actinides				MOX[a]	115–216	7.5–8.7
19		<20 MeV	^{238}U				MOX[b]	89–187	6.9–9.6
20		<20 MeV	Actinides				MOX[b]	109–218	7.7–9.8

[1] FTC Diff.(%) = $\frac{FTC_{SVV} - FTC_{BSM}}{FTC_{ASY}} \times 100$, see Eq. (8) for FTC.
[2] The FTC differences for each enrichment case were not individually documented.
[3] The difference in the Doppler reactivity coefficient were calculated manually and vary from the numbers reported in their paper.
[4] Based on Pu_2O_2 content of 4 wt.%, and 8 wt.% (their 20 wt.% cases was excluded due to a typo in their paper).
[5] The resonance integral data was calculated using their Monte Carlo Slowing Down code: MCSD code and supplied to CASMO-5.
[a] Reactor-Recycle MOX fuel.
[b] Weapons-Grade MOX fuel.

Formulation

Ousilomen and Sanchez, 1990:

$$\sigma_{sn}^T(E \to E') = \frac{\beta^{5/2}}{4E} e^{\frac{E}{kT}} \int_0^\infty t \sigma_s^{\mathsf{tab}}\left(\frac{\beta kT}{A} t^2\right) e^{-\frac{t^2}{A}} \Psi_n(t) dt$$

Formulation

Ousilomen and Sanchez, 1990:

$$\sigma_{sn}^{T}(E \to E') = \frac{\beta^{5/2}}{4E} e^{\frac{E}{kT}} \int_0^\infty t\sigma_s^{\text{tab}} \left(\frac{\beta kT}{A} t^2\right) e^{-\frac{t^2}{A}} \Psi_n(t) dt$$

For isotropic scattering:

$$\sigma_{s_0, g \to g'}^{T} = \frac{1}{\delta_g \delta_g'} \int_{E_g}^{E_{g+1}} dE \int_{E_{g'}}^{E_{g'+1}} dE' \sigma_{s_0}^{T}(E \to E')$$

Formulation

Ousilomen and Sanchez, 1990:

$$\sigma_{sn}^T(E \to E') = \frac{\beta^{5/2}}{4E} e^{\frac{E}{kT}} \int_0^\infty t\sigma_s^{\text{tab}}\left(\frac{\beta kT}{A} t^2\right) e^{-\frac{t^2}{A}} \Psi_n(t) dt$$

For isotropic scattering:

$$\sigma_{s_0,g \to g'}^T = \frac{1}{\delta_g \delta_g'} \int_{E_g}^{E_{g+1}} dE \int_{E_{g'}}^{E_{g'+1}} dE' \sigma_{s_0}^T(E \to E')$$

For within group scattering:

$$\sigma_{s_0,g \to g'}^T = \frac{1}{\delta_g \delta_{g'}} \int_{E_g}^{E_{g+1}} dE \left\{ \int_{E_g}^{E} dE' \sigma_{s_0}^T(E \to E') + \int_{E}^{E_{g+1}} dE' \sigma_{s_0}^T(E \to E') \right\}$$

Multi-group implementation of the scattering kernel with $\delta_g < 10^{-3} eV$

$$\delta_g \to 0, \delta_{g'} \to 0 \Rightarrow \sigma^T_{s_0, g \to g'} \approx \sigma^T_{s_0}(\overline{E}_g \to \overline{E}_{g'});$$
$$\overline{E}_g, \overline{E}_{g'} = \frac{E_{g+1} + E_g}{2}, \frac{E_{g'+1} + E_{g'}}{2}$$
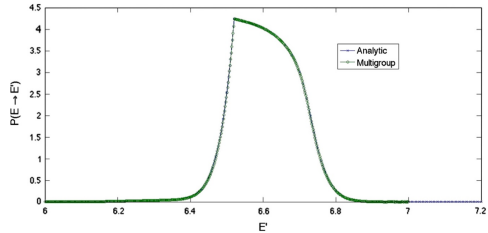
Fig. 1. Scattering kernel of ^{238}U at 1000 K for neutron starting at energy 6.52 eV.

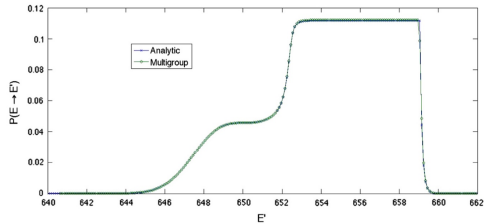**Fig. 2.** Scattering kernel of ^{238}U at 1000 K for neutron starting energy of 659.05 eV.
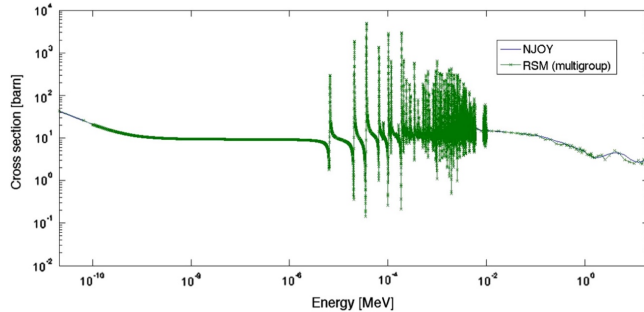
Fig. 3. The elastic cross section for ^{238}U at 900 K comparing NJOY multi-group results with those of the RSM using the same energy group structure.

- Using DRAGON Code, Marleau et al., 2010

- Using DRAGON Code, Marleau et al., 2010
- Scattering matrices generated with RSM calculation combined with NJOY data

- Using DRAGON Code, Marleau et al., 2010
- Scattering matrices generated with RSM calculation combined with NJOY data
- Fuel temperature coefficient:

$$FTC = \left(\frac{1}{k_{HZP}} - \frac{1}{k_{HFP}} \right) \frac{1 \times 10^5}{\Delta T}$$

Table 2
Fuel temperature coefficients for the Mosteller UOX benchmark with uranium enrichments ranging from 0.711% to 5.0% and the RSM kernel applied only to ^{238}U.

wt (%)	k (asymptotic kernel)			k (RSM kernel only for ^{238}U)			FTC diff (%)
	HZP	HFP	FTC	HZP	HFP	FTC	
0.711	0.6621394	0.6560206	−4.70	0.6614598	0.6548324	−5.10	−8.62
1.6	0.9562254	0.9478355	−3.09	0.9553188	0.9461777	−3.37	−9.25
2.4	1.0939660	1.0847290	−2.59	1.0929660	1.0828760	−2.84	−9.52
3.1	1.1716930	1.1620540	−2.36	1.1706490	1.1601060	−2.59	−9.66
3.9	1.2341210	1.2242040	−2.19	1.2330470	1.2221950	−2.40	−9.70
4.5	1.2694110	1.2593600	−2.10	1.2683240	1.2573230	−2.30	−9.72
5.0	1.2936360	1.2835050	−2.03	1.2925430	1.2814540	−2.23	−9.72

Table 3

Fuel temperature coefficients for the Mosteller UOX benchmark with uranium enrichments ranging from 0.711% to 5.0% and the RSM kernel applied for all the heavy nuclei.

wt (%)	k (RSM kernel for all uranium nuclei)			FTC diff (%)
	HZP	HFP	FTC	
0.711	0.6614576	0.6548296	−5.10	−8.63
1.6	0.9553133	0.9461702	−3.37	−9.27
2.4	1.0929570	1.0828640	−2.84	−9.56
3.1	1.1706380	1.1600910	−2.59	−9.70
3.9	1.2330470	1.2221950	−2.40	−9.70
4.5	1.2683090	1.2573000	−2.30	−9.81
5.0	1.2925260	1.2814290	−2.23	−9.81

Table 4
Fuel temperature coefficients for the Mosteller Reactor-Recycle MOX fuel benchmark with 1–8 wt.% PuO$_2$ and the RSM kernel applied to all the heavy nuclei.

MOX composition (PuO$_2$ wt.%)	k (asymptotic kernel)			k (RSM kernel)			FTC diff. (%)
	HZP	HFP	FTC	HZP	HFP	FTC	
1.0	0.9407429	0.9312128	−3.63	0.9395729	0.9292448	−3.94	−8.74
2.0	1.0183990	1.0076460	−3.49	1.0171230	1.0055030	−3.79	−8.43
4.0	1.0759170	1.0644960	−3.32	1.0746340	1.0623330	−3.59	−8.05
6.0	1.1057560	1.0942010	−3.18	1.1045310	1.0921170	−3.43	−7.76
8.0	1.1297120	1.1181500	−3.05	1.1285580	1.1161660	−3.28	−7.48

Table 5
Fuel temperature coefficients for the Mosteller Weapons-Grade MOX fuel benchmark with 1–6 wt.% PuO$_2$ and the RSM kernel applied to all the heavy nuclei.

MOX composition (PuO$_2$ wt.%)	k (asymptotic kernel)			k (RSM kernel)			FTC diff. (%)
	HZP	HFP	FTC	HZP	HFP	FTC	
1.0	1.0838630	1.0748170	−2.59	1.0827770	1.0728730	−2.84	−9.79
2.0	1.1765110	1.1656680	−2.64	1.1753040	1.1635420	−2.87	−8.79
4.0	1.2472990	1.2352440	−2.61	1.2460520	1.2330640	−2.82	−8.04
6.0	1.2847710	1.2725020	−2.50	1.2835640	1.2703840	−2.69	−7.71

Table 6
Fuel temperature coefficients for the Mosteller Reactor-Recycle MOX fuel benchmark with 1–8 wt.% PuO$_2$ and the RSM kernel applied to ^{238}U only.

MOX composition (PuO$_2$ wt.%)	HZP	HFP	FTC	FTC diff. (%)
1.0	0.9398723	0.9296191	−3.91	−7.87
2.0	1.0175060	1.0059940	−3.75	−7.33
4.0	1.0750620	1.0628910	−3.55	−6.81
6.0	1.1049570	1.0926810	−3.39	−6.46
8.0	1.1289670	1.1167140	−3.24	−6.18

Table 7
Fuel temperature coefficients for the Mosteller Weapons-Grade MOX fuel benchmark with 1–6 wt.% PuO$_2$ and the RSM kernel applied to ^{238}U only.

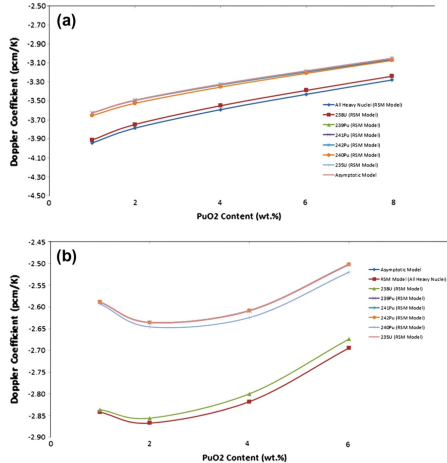| MOX composition (PuO$_2$ wt.%)	HZP	HFP	FTC	FTC diff. (%)
1.0	1.0828870	1.0730010	−2.84	−9.57
2.0	1.1755180	1.1637980	−2.86	−8.35
4.0	1.2463530	1.2334410	−2.80	−7.35
6.0	1.2838850	1.2707980	−2.67	−6.88

Fig. 4. Fuel temperature coefficient for the (a) Reactor-Recycle MOX fuel pin and (b) Weapons-Grade MOX fuel pin when applying the RSM to individual nuclei.

Table 8
The up-scattering percentage contribution of each nucleus towards the eigenvalue for Mosteller Reactor-Recycle MOX fuel benchmark with 1–8 wt.% PuO_2 at 600 K.

MOX composition (PuO_2 wt.%)	^{238}U	^{235}U	^{239}Pu	^{240}Pu	^{241}Pu	^{242}Pu
1.0	74.51	0.09	0.04	2.59	22.58	0.19
2.0	70.15	0.16	0.08	6.13	23.33	0.16
4.0	66.85	0.39	0.23	11.65	20.72	0.16
6.0	65.60	0.49	0.33	15.19	18.23	0.16
8.0	64.84	0.78	0.52	17.75	15.93	0.17

Table 9
The up-scattering percentage contribution of each nucleus towards the eigenvalue for Mosteller Reactor-Recycle MOX fuel benchmark with 1–8 wt.% PuO_2 at 900 K.

MOX composition (PuO_2 wt.%)	^{238}U	^{235}U	^{239}Pu	^{240}Pu	^{241}Pu	^{242}Pu
1.0	81.17	0.07	0.03	1.65	16.95	0.14
2.0	77.30	0.14	0.09	4.07	18.25	0.14
4.0	74.62	0.28	0.14	8.00	16.83	0.14
6.0	73.54	0.39	0.24	10.64	15.05	0.15
8.0	73.12	0.56	0.31	12.53	13.39	0.10

Table 10
The up-scattering percentage contribution of each nucleus towards the eigenvalue for Mosteller Weapons-Grade MOX fuel benchmark with 1–6 wt.% PuO_2 at 600 K.

MOX composition (PuO_2 wt.%)	^{238}U	^{235}U	^{239}Pu	^{240}Pu	^{241}Pu	^{242}Pu
1.0	89.87	0.18	0.00	0.00	9.76	0.18
2.0	82.41	0.33	0.00	0.00	17.10	0.17
4.0	75.98	0.64	0.00	0.00	23.21	0.16
6.0	73.59	0.91	0.00	0.00	25.33	0.17

Table 11
The up-scattering percentage contribution of each nucleus towards the eigenvalue for Mosteller Weapons-Grade MOX fuel benchmark with 1–6 wt.% PuO_2 at 900 K.

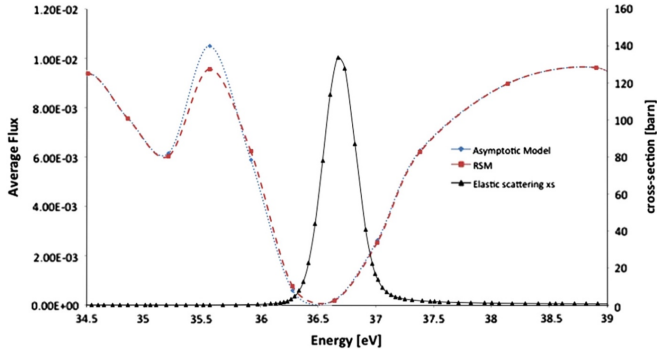| MOX composition (PuO_2 wt.%)	^{238}U	^{235}U	^{239}Pu	^{240}Pu	^{241}Pu	^{242}Pu
1.0	93.51	0.15	0.00	0.00	6.18	0.15
2.0	88.08	0.28	0.00	0.00	11.49	0.14
4.0	82.90	0.51	0.00	0.00	16.46	0.14
6.0	80.80	0.71	0.00	0.00	18.40	0.09

Fig. 5. Neutron flux of the fuel region for UO$_2$ pin-cell at 0.711 wt.% enrichment at 600 K near the third resonances of ^{238}U, 36.68 eV, using the RSM (dashed curve) and the traditional asymptotic (dotted curve) model. The elastic scattering cross section is also plotted (solid curve).
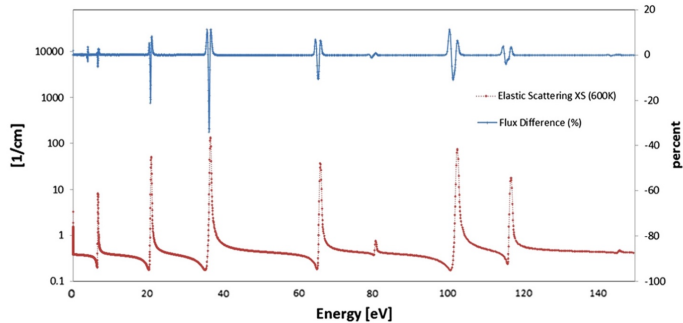
Fig. 6. Relative difference in flux (%, solid curve above) between the asymptotic model and the resonance scattering model plotted against the macroscopic cross-section of the fuel (dotted curve below). Where the flux is almost zero, the relative error is very large (which cannot be seen in Fig. 5 due to the scale in that figure).
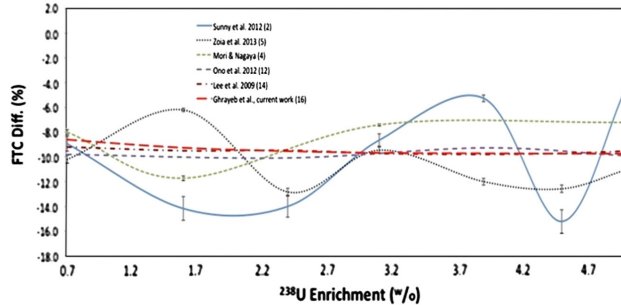
Fig. 7. Comparison of the FTC differences for UOX Mosteller benchmark. The results of Ghrayeb et al. (long dashed curve) and Lee et al. 2009 (dash dot curve) compare relatively well against each other showing a nearly constant behavior in FTC difference with respect to ^{235}U enrichment. However, there is no consensus among the work of others to show consistency in FTC difference with respect to ^{235}U enrichment. The numbers in parentheses correspond to the first column of Table 1.

- Temperature-dependent resonance scattering and up scattering effects are considered in slowing down calculation.

- Temperature-dependent resonance scattering and up scattering effects are considered in slowing down calculation.
- Asymptotic model for neutron-nuclei elastic scattering under predicts the Dopler coefficient by as much as 10% in LWR lattices.

- Temperature-dependent resonance scattering and up scattering effects are considered in slowing down calculation.
- Asymptotic model for neutron-nuclei elastic scattering under predicts the Dopler coefficient by as much as 10% in LWR lattices.
- In the case of the UO_2 fuel, the contribution of up-scattering was overwhelmingly due to ^{238}U.

- Temperature-dependent resonance scattering and up scattering effects are considered in slowing down calculation.
- Asymptotic model for neutron-nuclei elastic scattering under predicts the Dopler coefficient by as much as 10% in LWR lattices.
- In the case of the UO_2 fuel, the contribution of up-scattering was overwhelmingly due to ^{238}U.
- When using RSM instead of asymptotic model, in case of UO_2 fuel, change in eigenvalues varies from 68 to 208 pcm.

Summary of Main Aspects, TLDR

▶ Temperature-dependent resonance scattering and up scattering effects are considered in slowing down calculation.

▶ Asymptotic model for neutron-nuclei elastic scattering under predicts the Dopler coefficient by as much as 10% in LWR lattices.

▶ In the case of the UO_2 fuel, the contribution of up-scattering was overwhelmingly due to ^{238}U.

▶ When using RSM instead of asymptotic model, in case of UO_2 fuel, change in eigenvalues varies from 68 to 208 pcm.

▶ In the case of the weapons-grade MOX fuel the largest and most significant contribution to resonance up-scattering after that of ^{238}U is that of ^{241}Pu, which is responsible for as much as 25% of up-scattering

Thanks!
Questions?